

# Mapping the Specific Amino Acid Residues That Make Hamster DPP4 Functional as a Receptor for Middle East Respiratory Syndrome Coronavirus

Neeltje van Doremalen, Kerri L. Miazgowicz,\* Vincent J. Munster

Laboratory of Virology, Division of Intramural Research, National Institute of Allergy and Infectious Diseases, National Institutes of Health, Hamilton, Montana, USA

## ABSTRACT

The novel emerging coronavirus Middle East respiratory syndrome coronavirus (MERS-CoV) binds to its receptor, dipeptidyl peptidase 4 (DPP4), via 14 interacting amino acids. We previously showed that if the five interacting amino acids which differ between hamster and human DPP4 are changed to the residues found in human DPP4, hamster DPP4 does act as a receptor. Here, we show that the functionality of hamster DPP4 as a receptor is severely decreased if less than 4 out of 5 amino acids are changed.

## IMPORTANCE

The novel emerging coronavirus MERS-CoV has infected >1,600 people worldwide, and the case fatality rate is ~36%. In this study, we show that by changing 4 amino acids in hamster DPP4, this protein functions as a receptor for MERS-CoV. This work is vital in the development of new small-animal models, which will broaden our understanding of MERS-CoV and be instrumental in the development of countermeasures.

Middle East respiratory syndrome coronavirus (MERS-CoV) has been detected in >1,600 patients, and the case fatality rate is 36%. Although the majority of cases have occurred in Saudi Arabia (80%), an outbreak in South Korea sparked by a patient with a history of travel in the Middle East highlights the potential for MERS-CoV to be transmitted via the nosocomial route if no appropriate measures are taken (1). MERS-CoV has an unusual broad host tropism that includes humans and dromedary camels. A better understanding of the molecular basis of the host tropism will help determine the restrictions of potential host species and improve the functional design of animal models and the development of medical countermeasures. Several animal models for MERS-CoV have been developed. Nonhuman primates (NHPs) (2–4) and dromedary camels (5) are naturally susceptible. In addition, several mouse models have been developed, and expression of the human variant of the receptor of MERS-CoV, dipeptidyl peptidase 4 (DPP4), in mice allows viral replication (6–8). No other small-animal models have been developed. Therefore, if a treatment against MERS-CoV is shown to be successful in the mouse model, further characterization of the treatment needs to be performed in NHPs, a relatively expensive animal model to which access is limited. The availability of a second small-animal model (such as hamsters with a modified DPP4 [9, 10]) to confirm results obtained with the mouse model would ensure that only treatments with a high likelihood of succeeding would be investigated in NHPs.

Fourteen amino acids are important in the interaction between blades IV and V of human DPP4 (hDPP4) and the receptor binding domain (RBD) of the MERS-CoV spike protein (11, 12). We previously showed that hamster DPP4 (haDPP4) does not function as a receptor for MERS-CoV. This restriction is caused by 5 out of 14 interacting amino acids which differ between hDPP4 and haDPP4 (Fig. 1) (13). In the study described here, we analyzed the minimal combination of these 5 amino acids (aa) allowing haDPP4 to function as a receptor for MERS-CoV.

## MATERIALS AND METHODS

**Biosafety statement.** All experiments performed with MERS-CoV were done in a high-containment facility at the Rocky Mountain Laboratories (RML), Division of Intramural Research (DIR), National Institute of Allergy and Infectious Diseases (NIAID), National Institutes of Health (NIH). The work was approved by RML Institutional Biosafety Committee (IBC) at biosafety level 3 (BSL3).

**Cells and virus.** Baby hamster kidney (BHK) cells were maintained in Dulbecco's modified Eagle's medium (DMEM) supplemented with 10% fetal bovine serum (FBS), 2 mM L-glutamine, 50 U/ml penicillin, and 50 µg/ml of streptomycin (culture DMEM) and maintained at 37°C in 5% CO<sub>2</sub>. MERS-CoV (strain HCoV-EMC/2012) was propagated on Vero E6 cells using DMEM supplemented with 2% FBS, 2 mM L-glutamine, 50 U/ml penicillin, and 50 µg/ml of streptomycin (complete DMEM). MERS-CoV was titrated by endpoint titration in quadruplicate on Vero E6 cells cultured in complete DMEM as follows: cells were inoculated with 10-fold serial dilutions of virus and scored for the cytopathic effect 5 days later. The 50% tissue culture infective dose (TCID<sub>50</sub>) was calculated by the Spearman-Kärber method (14).

**Plasmids and transfection of BHK cells.** Mutagenized DPP4 in expression plasmid pcDNA3.1(+) was generated using a QuikChange Lightning site-directed mutagenesis kit (Agilent). The modifications to the DPP4 sequences were confirmed by Sanger sequencing. Baby hamster

Received 30 December 2015 Accepted 18 March 2016

Accepted manuscript posted online 30 March 2016

**Citation** van Doremalen N, Miazgowicz KL, Munster VJ. 2016. Mapping the specific amino acid residues that make hamster DPP4 functional as a receptor for Middle East respiratory syndrome coronavirus. *J Virol* 90:5499–5502. doi:10.1128/JVI.03267-15.

**Editor:** A. García-Sastre, Icahn School of Medicine at Mount Sinai

Address correspondence to Vincent J. Munster, vincent.munster@nih.gov.

\* Present address: Kerri L. Miazgowicz, Department of Infectious Diseases, College of Veterinary Medicine, University of Georgia, Athens, Georgia, USA.

Copyright © 2016, American Society for Microbiology. All Rights Reserved.

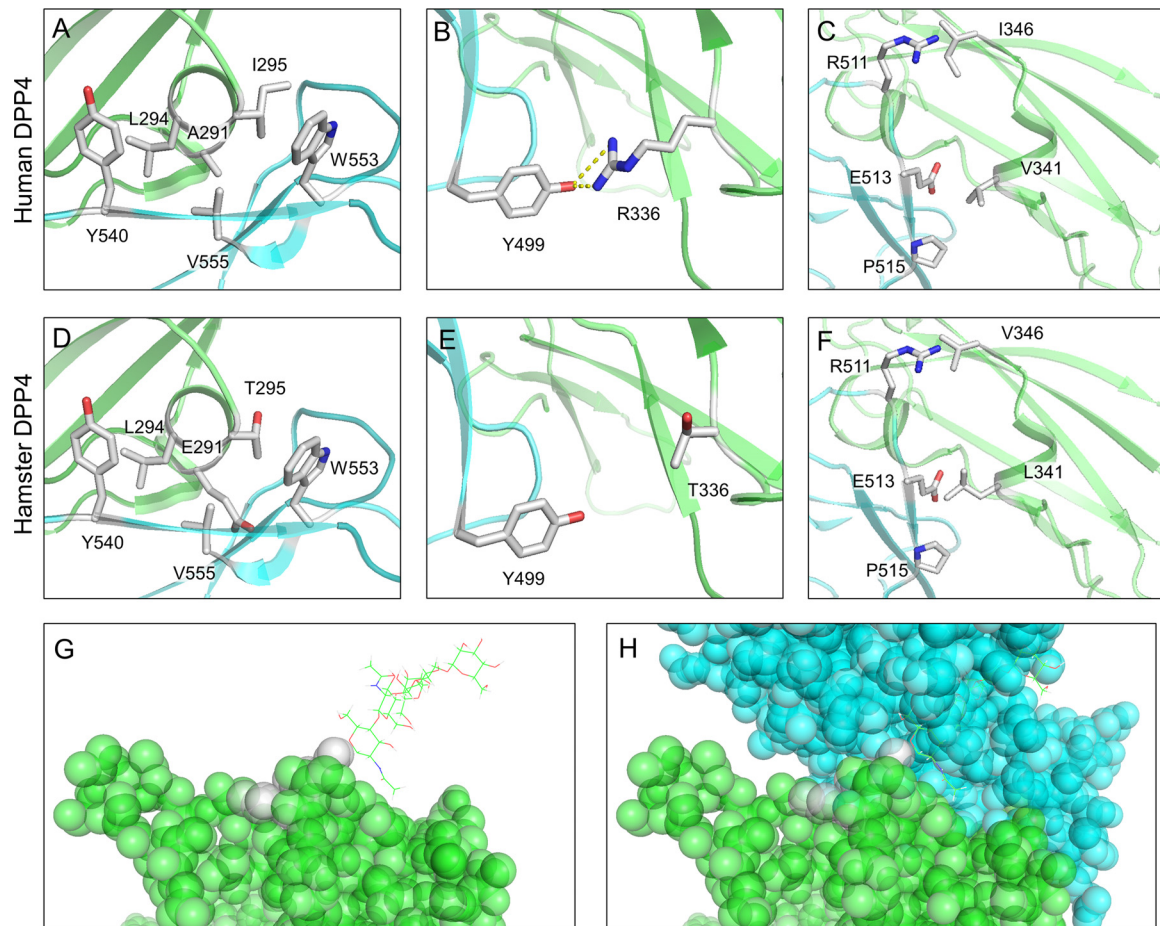


**FIG 1** Interaction between the MERS-CoV RBD and DPP4. (A to F) Cartoon of detailed interactions between MERS-CoV residues and human (A to C) or hamster (D to F) DPP4 residues. (G to H) Cartoon of the predicted blockade of MERS-CoV RBD binding by glycosylation of the motif from residues 334 to 336 of hamster DPP4. Green, DPP4; cyan, MERS-CoV RBD; gray, interacting amino acid (A to F) or the glycosylation site (G and H).

kidney cells were transfected with 3  $\mu$ g pcDNA3.1(+) containing the DPP4 genes using 8  $\mu$ l of the Lipofectamine 2000 reagent (Life Technologies). DPP4 expression was confirmed via flow cytometry.

**Flow cytometry.** Transfected BHK cells were removed with 5 mM EDTA, resuspended in phosphate-buffered saline with 2% FBS, and stained at 4°C using anti-human DPP4 antibody (catalog number AF1180; R&D Systems), followed by staining with fluorescein isothiocyanate-tagged donkey anti-goat immunoglobulin antibody (catalog number A11055; Life Technologies). As a control, samples of cells were stained with secondary antibody only. Only viable cells were selected using 7-aminocinomycin D (Life Technologies). Samples were collected using an LSR II flow cytometer (BD Biosciences). Ten thousand gated events were analyzed for each sample. Data were analyzed using FlowJo software (TreeStar), with the data for transfected BHK cells being compared with those for untransfected BHK cells.

**Virus replication kinetics.** Multistep replication kinetics were determined by inoculating cells with MERS-CoV at a multiplicity of infection (MOI) of 1 TCID<sub>50</sub> per cell. At 1 h after inoculation, the cells were washed twice with DMEM and fresh complete DMEM was placed on the cells. The supernatants were sampled at 0, 24, 48, and 72 h after inoculation, and the virus titers in these supernatants were determined as described above. All experiments were done in triplicate. The mean viral titer and standard deviation were determined for each condition.

**Image design.** Three-dimensional images were created using the structure with PDB accession number 4KR0 and the DPP4 sequence from

GenBank with accession number [KF574266.1](https://www.ncbi.nlm.nih.gov/nuccore/KF574266.1) in PyMOL software (v1.8) (15).

## RESULTS

The contribution of individual amino acids was investigated by MERS-CoV infection of BHK cells transfected with haDPP4 containing single amino acid substitutions representing the human DPP4 sequence (Fig. 2A and Table 1). None of the mutant haDPP4 variants with single amino acid substitutions representing the human DPP4 sequence was able to support MERS-CoV replication. Next, BHK cells were transfected with hDPP4 containing single amino acid substitutions representing the hamster DPP4 sequence (Fig. 2B). The substitutions A291E and R336T in hDPP4 abrogated MERS-CoV replication completely. Amino acid substitution I295T reduced viral growth slightly compared to that of wild-type virus in cells transfected with human DPP4. Expression of the other single amino acid substitutions (V341L and I346V) resulted in virus titers similar to those from BHK cells transfected with wild-type hDPP4. Then, the following three double mutants and one triple mutant with a backbone of haDPP4 and amino acids of human DPP4 were constructed: E291A and T295I; E291A and T336R; T295I and T336R; and E291A, T295I, and T336R. Expression of mutants with these mutations on BHK

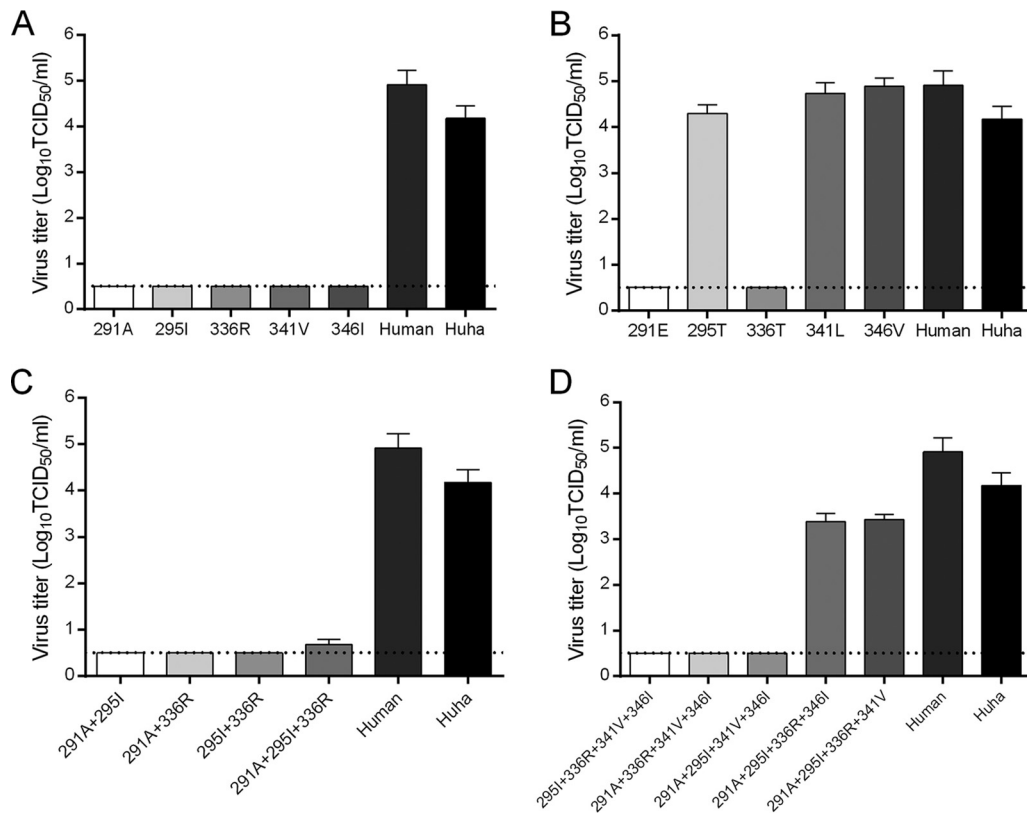


**FIG 2** MERS-CoV replication in BHK cells expressing variants of DPP4. TCID<sub>50</sub> values were measured at 72 h postinfection. The designation(s) below the bars represents the amino acid changed to the human or hamster variant. (A) BHK cells were transfected with DPP4 of hamster origin with a single mutation to an amino acid representing human DPP4; (B) BHK cells were transfected with DPP4 of human origin with a single mutation to an amino acid representing hamster DPP4; (C) BHK cells were transfected with DPP4 of hamster origin with double or triple mutations to amino acids representing human DPP4; (D) BHK cells were transfected with DPP4 of hamster origin with quadruple mutations to amino acids representing human DPP4. Mean viral titers were calculated from three independent experiments. Error bars indicate standard deviations. Huha, humanized hamster.

cells did not result in MERS-CoV replication (Fig. 2C). Finally, the functionality of haDPP4 with four out of five residues of human DPP4 was investigated. Attenuated MERS-CoV replication was measured when cells expressed fully humanized haDPP4 except for residue 341V or 346I (Fig. 2D).

## DISCUSSION

We show that all of the five interacting residues that differ between hDPP4 and haDPP4 are important in the binding of the MERS-CoV spike protein. This is in contrast to murine DPP4, where mutagenesis of two out of five (L294A and R336T) interacting residues to the amino acids found in human DPP4 resulted in MERS-CoV replication similar to that achieved with hDPP4 (~1 log unit lower) (16).

Of the five residues important in haDPP4, residues 291 and 336 were found to be the most critical, followed by residue 295, whereas residues 341 and 346 were found to be the least critical. In hDPP4, residues A291, L294, and I295 form a hydrophobic core with RBD residues surrounded by a hydrophilic periphery (11). In contrast, haDPP4 contains a hydrophilic residue at position 291 (E) and a neutral residue at position 295 (T), theoretically destroying the hydrophobic pocket. Indeed, residue E291 was found to be abortive for binding in both backbones, whereas residue T295 had a moderate effect on RBD-DPP4 binding. Likewise, residue 295

was found to be less important in the binding of murine DPP4 by the MERS-CoV RBD (17).

haDPP4 is predicted to contain a glycosylation site at position 336 which is absent in hDPP4 and which is predicted to interfere with RBD binding (17). This is reflected in the observed lack of viral replication when DPP4 contains the residue from hamster DPP4 at position 336.

Finally, hDPP4 V341 and I346 form small hydrophobic patches with RBD residues, and these are replaced by L341 and V346 in haDPP4. These residues have properties very similar to those of the residues in hDPP4, and the presence of these residues results in minimum attenuation of binding. Although residues 341 and 346 have an effect on RBD binding in the background of haDPP4, this effect is much less critical than the interaction between RBD and residues 291, 295, and 336.

We observed a difference in outcome when using haDPP4 or hDPP4 as a backbone when investigating residues 295, 341, and 346; changes that have a negligible effect on hDPP4 and RBD binding can be measured as an attenuation of viral replication when using an haDPP4 background, reflecting suboptimal receptor binding.

In order to utilize the hamster as an animal model for MERS-CoV infection, all 5 aa involved in host restriction need to be changed to the hDPP4 equivalents in order to optimize the inter-

TABLE 1 Summary of mutated DPP4 proteins and the ability to function as a MERS-CoV receptor<sup>a</sup>

| Backbone | Amino acid residue at position: |          |          |          |          | Viral growth | No. of TCID <sub>50</sub> s at 72 hpi |
|----------|---------------------------------|----------|----------|----------|----------|--------------|---------------------------------------|
|          | 291                             | 295      | 336      | 341      | 346      |              |                                       |
| Human    | <b>A</b>                        | <b>I</b> | <b>R</b> | <b>V</b> | <b>I</b> | +/+          | 8.1 × 10 <sup>4</sup>                 |
| Hamster  | <i>E</i>                        | <i>T</i> | <i>T</i> | <i>L</i> | <i>V</i> | -/-          | <DL                                   |
| Hamster  | <b>A</b>                        | <i>T</i> | <i>T</i> | <i>L</i> | <i>V</i> | -/-          | <DL                                   |
| Hamster  | <i>E</i>                        | <b>I</b> | <i>T</i> | <i>L</i> | <i>V</i> | -/-          | <DL                                   |
| Hamster  | <i>E</i>                        | <i>T</i> | <b>R</b> | <i>L</i> | <i>V</i> | -/-          | <DL                                   |
| Hamster  | <i>E</i>                        | <i>T</i> | <i>T</i> | <b>V</b> | <i>V</i> | -/-          | <DL                                   |
| Hamster  | <i>E</i>                        | <i>T</i> | <i>T</i> | <i>L</i> | <b>I</b> | -/-          | <DL                                   |
| Hamster  | <b>A</b>                        | <b>I</b> | <i>T</i> | <i>L</i> | <i>V</i> | -/-          | <DL                                   |
| Hamster  | <b>A</b>                        | <i>T</i> | <b>R</b> | <i>L</i> | <i>V</i> | -/-          | <DL                                   |
| Hamster  | <i>E</i>                        | <b>I</b> | <b>R</b> | <i>L</i> | <i>V</i> | -/-          | <DL                                   |
| Hamster  | <b>A</b>                        | <b>I</b> | <b>R</b> | <i>L</i> | <i>V</i> | -/-          | 5 × 10 <sup>0</sup>                   |
| Hamster  | <i>E</i>                        | <b>I</b> | <b>R</b> | <b>V</b> | <b>I</b> | -/-          | <DL                                   |
| Hamster  | <b>A</b>                        | <i>T</i> | <b>R</b> | <b>V</b> | <b>I</b> | -/-          | <DL                                   |
| Hamster  | <b>A</b>                        | <b>I</b> | <i>T</i> | <b>V</b> | <b>I</b> | -/-          | <DL                                   |
| Hamster  | <b>A</b>                        | <b>I</b> | <b>R</b> | <i>L</i> | <b>I</b> | +/-          | 2.4 × 10 <sup>3</sup>                 |
| Hamster  | <b>A</b>                        | <b>I</b> | <b>R</b> | <b>V</b> | <i>V</i> | +/-          | 2.7 × 10 <sup>3</sup>                 |
| Human    | <i>E</i>                        | <b>I</b> | <b>R</b> | <b>V</b> | <b>I</b> | -/-          | <DL                                   |
| Human    | <b>A</b>                        | <i>T</i> | <b>R</b> | <b>V</b> | <b>I</b> | +/-          | 2.0 × 10 <sup>4</sup>                 |
| Human    | <b>A</b>                        | <b>I</b> | <i>T</i> | <b>V</b> | <b>I</b> | -/-          | <DL                                   |
| Human    | <b>A</b>                        | <b>I</b> | <b>R</b> | <i>L</i> | <b>I</b> | +/+          | 5.4 × 10 <sup>4</sup>                 |
| Human    | <b>A</b>                        | <b>I</b> | <b>R</b> | <b>V</b> | <i>V</i> | +/+          | 7.7 × 10 <sup>4</sup>                 |

<sup>a</sup> hpi, hours postinfection; boldface, human residues; italics, hamster residues; +/+, viral growth; +/-, attenuated viral growth; -/-, no viral growth; <DL, below the detection limit of the assay.

action between the receptor and the virus. Adaptation of MERS-CoV to haDPP4 is predicted to be unsuccessful, due to the glycosylation site at positions 334 to 336. Descriptions of transgenic hamsters are virtually absent from the scientific literature due to the absence of specific gene-targeting tools. Utilization of the clustered regularly interspaced short palindromic repeat (CRISPR)/Cas9 system would allow efficient gene targeting and the generation of a new small-animal model (9, 10).

## ACKNOWLEDGMENTS

We thank Bart Haagmans and Ron Fouchier for providing pcDNA3.1(+) human DPP4 and HCoV-EMC/2012, Rebekah McMinn and Jacob Conroy for assistance with the figures, and Aaron Carmody for assistance with the flow cytometry.

## FUNDING INFORMATION

This work, including the efforts of Neeltje van Doremalen, Kerri Miazgowiec, and Vincent J. Munster, was funded by Division of Intramural Research, National Institute of Allergy and Infectious Diseases (DIR, NIAID).

This research was supported by the Intramural Research Program of the National Institute of Allergy and Infectious Diseases (NIAID), National Institutes of Health (NIH).

## REFERENCES

1. WHO. Middle East respiratory syndrome coronavirus. WHO, Geneva, Switzerland. <http://www.who.int/emergencies/mers-cov/en/>.
2. Falzarano D, de Wit E, Feldmann F, Rasmussen AL, Okumura A, Peng X, Thomas MJ, van Doremalen N, Haddock E, Nagy L, LaCasse R, Liu T, Zhu J, McLellan JS, Scott DP, Katze MG, Feldmann H, Munster VJ. 2014. Infection with MERS-CoV causes lethal pneumonia in the common marmoset. *PLoS Pathog* 10:e1004250. <http://dx.doi.org/10.1371/journal.ppat.1004250>.
3. de Wit E, Rasmussen AL, Falzarano D, Bushmaker T, Feldmann F, Brining DL, Fischer ER, Martellaro C, Okumura A, Chang J, Scott D, Benecke AG, Katze MG, Feldmann H, Munster VJ. 2013. Middle East respiratory syndrome coronavirus (MERS-CoV) causes transient lower respiratory tract infection in rhesus macaques. *Proc Natl Acad Sci U S A* 110:16598–16603. <http://dx.doi.org/10.1073/pnas.1310744110>.
4. Yao Y, Bao L, Deng W, Xu L, Li F, Lv Q, Yu P, Chen T, Xu Y, Zhu H, Yuan J, Gu S, Wei Q, Chen H, Yuen KY, Qin C. 2014. An animal model of MERS produced by infection of rhesus macaques with MERS coronavirus. *J Infect Dis* 209:236–242. <http://dx.doi.org/10.1093/infdis/jit590>.
5. Adney DR, van Doremalen N, Brown VR, Bushmaker T, Scott D, de Wit E, Bowen RA, Munster VJ. 2014. Replication and shedding of MERS-CoV in upper respiratory tract of inoculated dromedary camels. *Emerg Infect Dis* 20:1999–2005. <http://dx.doi.org/10.3201/eid2012.141280>.
6. Zhao J, Li K, Wohlford-Lenane C, Agnihothram SS, Fett C, Zhao J, Gale MJ, Jr, Baric RS, Enjuanes L, Gallagher T, McCray PB, Jr, Perlman S. 2014. Rapid generation of a mouse model for Middle East respiratory syndrome. *Proc Natl Acad Sci U S A* 111:4970–4975. <http://dx.doi.org/10.1073/pnas.1323279111>.
7. Agrawal AS, Garron T, Tao X, Peng BH, Wakamiya M, Chan TS, Couch RB, Tseng CT. 2015. Generation of a transgenic mouse model of Middle East respiratory syndrome coronavirus infection and disease. *J Virol* 89:3659–3670. <http://dx.doi.org/10.1128/JVI.03427-14>.
8. Pascal KE, Coleman CM, Mujica AO, Kamat V, Badithe A, Fairhurst J, Hunt C, Strein J, Berrebi A, Sisk JM, Matthews KL, Babb R, Chen G, Lai KM, Huang TT, Olson W, Yancopoulos GD, Stahl N, Frieman MB, Kyratsous CA. 2015. Pre- and postexposure efficacy of fully human antibodies against spike protein in a novel humanized mouse model of MERS-CoV infection. *Proc Natl Acad Sci U S A* 112:8738–8743. <http://dx.doi.org/10.1073/pnas.1510830112>.
9. Fan Z, Li W, Lee SR, Meng Q, Shi B, Bunch TD, White KL, Kong IK, Wang Z. 2014. Efficient gene targeting in golden Syrian hamsters by the CRISPR/Cas9 system. *PLoS One* 9:e109755. <http://dx.doi.org/10.1371/journal.pone.0109755>.
10. Gao M, Zhang B, Liu J, Guo X, Li H, Wang T, Zhang Z, Liao J, Cong N, Wang Y, Yu L, Zhao D, Liu G. 2014. Generation of transgenic golden Syrian hamsters. *Cell Res* 24:380–382. <http://dx.doi.org/10.1038/cr.2014.2>.
11. Lu G, Hu Y, Wang Q, Qi J, Gao F, Li Y, Zhang Y, Zhang W, Yuan Y, Bao J, Zhang B, Shi Y, Yan J, Gao GF. 2013. Molecular basis of binding between novel human coronavirus MERS-CoV and its receptor CD26. *Nature* 500:227–231. <http://dx.doi.org/10.1038/nature12328>.
12. Wang N, Shi X, Jiang L, Zhang S, Wang D, Tong P, Guo D, Fu L, Cui Y, Liu X, Arledge KC, Chen YH, Zhang L, Wang X. 2013. Structure of MERS-CoV spike receptor-binding domain complexed with human receptor DPP4. *Cell Res* 23:986–993. <http://dx.doi.org/10.1038/cr.2013.92>.
13. van Doremalen N, Miazgowiec KL, Milne-Price S, Bushmaker T, Robertson S, Scott D, Kinne J, McLellan JS, Zhu J, Munster VJ. 2014. Host species restriction of Middle East respiratory syndrome coronavirus through its receptor, dipeptidyl peptidase 4. *J Virol* 88:9220–9232. <http://dx.doi.org/10.1128/JVI.00676-14>.
14. Finney DJ. 1964. Statistical method in biological assay. Hafner Publishing Co, New York, NY.
15. Schrödinger. The PyMOL molecular graphics system, v1.7.4. Schrödinger, New York, NY.
16. Cockrell AS, Peck KM, Yount BL, Agnihothram SS, Scobey T, Curnes NR, Baric RS, Heise MT. 2014. Mouse dipeptidyl peptidase 4 is not a functional receptor for Middle East respiratory syndrome coronavirus infection. *J Virol* 88:5195–5199. <http://dx.doi.org/10.1128/JVI.03764-13>.
17. Peck KM, Cockrell AS, Yount BL, Scobey T, Baric RS, Heise MT. 2015. Glycosylation of mouse DPP4 plays a role in inhibiting Middle East respiratory syndrome coronavirus infection. *J Virol* 89:4696–4699. <http://dx.doi.org/10.1128/JVI.03445-14>.